Development of a passive blade-pitch mechanism to reduce the loads on a tidal turbine in high-flow conditions

Thomas Summers, Selda Oterkus, Gavin Tabor, Jonathan Shek, George Dadd and Bevan Wray

Abstract—**An initial design for a novel passive blade-pitch mechanism for a tidal turbine has been developed. This technology aims to reduce the loads on the rotor in high-flow conditions when compared to fixed-pitch blades, whilst reducing complexity and increasing reliability when compared to active pitch systems. This would enable larger rotor blades to be installed on turbines that currently employ fixed-pitch blades, without the capital or maintenance costs associated with active-pitch control. A fluid-structure interaction tool which couples the mechanical response of the passive-pitch mechanism with *NREL*'s *AeroDyn* blade element momentum code has been developed. Turbine performance has then been modelled for a range of operating conditions, allowing the influence of blade geometry, rotor diameter and passive-pitch characteristics to be analysed in terms of rotor loading and turbine performance. Initial analysis suggests that installing blades with a passive pitch mechanism could reduce the loads on the rotor in high-flow conditions down by 50% compared to the loads that would act on an equivalent rotor with fixed-pitch blades. This would allow larger diameter rotors to be installed, which could improve annual energy yield by 32.7% at a typical site.**

This work was supported by EPSRC and NERC under the InDustrial CDT in Offshore Renewable Energy programme.

T. Summers is a Research Engineer on the IDCORE programme, sponsored by Tocardo Ltd, Unit 3 Penstraze Business Centre, Penstraze, Truro, TR4 8PN, UK (e-mail: tom.summers@ed.ac.uk).

S. Oterkus is a professor of Naval Architecture, Ocean and Marine Engineering at University of Strathclyde at the University of Strathclyde, 100 Montrose Street, Glasgow, G4 0LZ, UK (e-mail: selda.oterkus@strath.ac.uk).

G. Tabor is a professor of Computational Fluid Dynamics at the University of Exeter, Harrison Building, Streatham Campus, University of Exeter, North Park Road, Exeter, EX4 4QF, UK (e-mail: G.R.Tabor@exeter.ac.uk).

J. Shek is the Deputy Head of the Institute for Energy Systems at the University of Edinburgh, School of Engineering, The University of Edinburgh, The King's Buildings, Mayfield Road, Edinburgh, EH9 3DW, UK (e-mail: jshek@ed.ac.uk).

G. Dadd is a Design Engineer at HydroWing Ltd, Unit 3 Penstraze Business Centre, Penstraze, Truro, TR4 8PN, UK (e-mail: gda@inyanga.tech).

B. Wray is a Project Engineer at HydroWing Ltd, Unit 3 Penstraze Business Centre, Penstraze, Truro, TR4 8PN, UK (e-mail: brw@inyanga.tech).

Digital Object Identifier: https://doi.org/10.36688/ewtec-2023-328

Keywords—**Fluid-structure interaction, load reduction, passive pitch control, tidal turbine.**

I. Introduction

TIDAL currents offer a predictable and sustainable source of energy, but the levelised cost of energy (LCOE) generated by tidal turbines remains significantly higher than other renewables. This is largely due to the fact that maintenance is expensive [1], and relies upon suitable weather conditions and vessel availability, which can lead to costly delays [2], [3].

Operation and maintenance (O&M) costs can be reduced by eliminating complex systems such as active blade-pitch control. LCOE for tidal turbines, however, depends upon both costs and energy yield [4]. Eliminating blade-pitch altogether by installing fixed-pitch blades reduces O&M costs, but necessitates the use of smaller rotor blades, which capture less energy from the tidal flow. This can result in an unviable LCOE, especially at low-flow sites, which are far more common than high-flow tidal sites [5].

The development of a passive blade-pitch mechanism to reduce the loads on a tidal turbine in high-flow conditions offers the potential to reduce complexity, and therefore maintenance costs, when compared to active pitch systems, whilst allowing larger blades to be installed, which will capture more energy when compared to fixed-pitch turbines.

A. Tidal turbine control methods

The aim of tidal turbine control is to enable the device to capture as much energy as possible in low-flow conditions, which occur most of the time, whilst ensuring that the turbine can survive less frequent high-flow conditions [6].

The control methods for tidal turbines can be categorised as follows: variable-speed fixed-pitch, constant-speed variable-pitch, or variable-speed variable-pitch.

Variable-speed control allows turbines to reduce the torque acting on the rotor in high-flow conditions by moving away from the peak on the torque coefficient curve [7]. For a rotor operating at a rotational speed, ω, tip speed ratio, λ, is the ratio of the speed of the blade tip,

at radius r_{tip}, to the free stream flow speed, U_∞, as shown in (1).

$$\lambda = \frac{r_{tip}\omega}{U_\infty} \quad (1)$$

Turbine rotors can therefore move away from the peak on the coefficient of torque curve, a typical example of which is shown in Fig. 1, by either increasing the rotational speed, which reduces the angle of attack along the span of the blade, or by reducing rotational speed such that the blade stalls [8].

Variable-pitch control allows turbines to respond to an increase in flow speed by increasing the blade pitch angle, β, as shown in Fig. 2, such that the leading edge rotates towards the direction of the freestream flow [6]. This is known as *pitch-to-feather*, and leads to a reduced angle of attack along the length of the blade, resulting in reduced coefficients of power and thrust in high flow speeds [9], as shown in Fig. 3. Variable-pitch control may or may not be used in conjunction with speed-control.

B. *Active pitch control*

Active pitch systems incorporate an actuator to provide the pitching moment, bearings to allow pitch rotation, an encoder to measure the blade pitch angle, and a controller based on a combination of proportional, integral and derivative feedback [10]–[13].

Active pitch systems allow any pitch angle to be targeted in any operating condition. The disadvantage of active pitch systems, however, is that they are complex and therefore require frequent maintenance, which, due to the inherent difficulties associated with tidal turbine access, drives up the LCOE [4], [14]. Active pitch systems employed on wind turbines have even been shown to be responsible for up to 27% of all failures, more than any other system on wind turbines [15]–[17]

C. *Passive pitch control*

Passive pitch mechanisms use either the hydrodynamic forces generated by the rotor blade, the centrifugal force generated by the rotation of the blade, or a combination of both, in order to cause the blades to *pitch-to-feather* in high-flow conditions.

A degree of passive blade-pitching has been shown to be achievable by exploiting the anisotropic properties of composite materials such that the bending moment developed by the hydrodynamic forces acting on the blade causes the blade to twist along its pitch axis [18]–[20]. This is known as *bend-twist coupling* and has been shown to offer a reduction of thrust load in high-flow conditions of up to 12%, without significantly affecting the power captured in low-flow conditions [18].

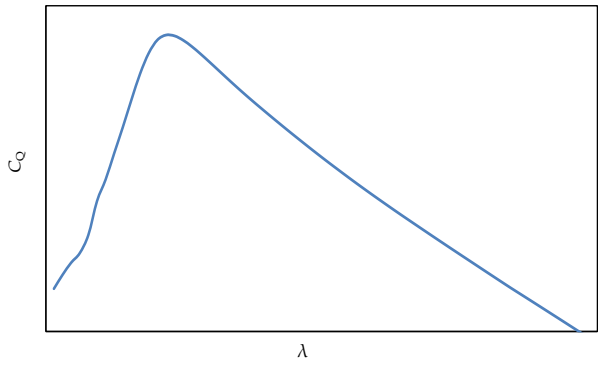

Fig. 1. Typical relationship between coefficient of torque, C_Q, and tip speed ratio, λ.

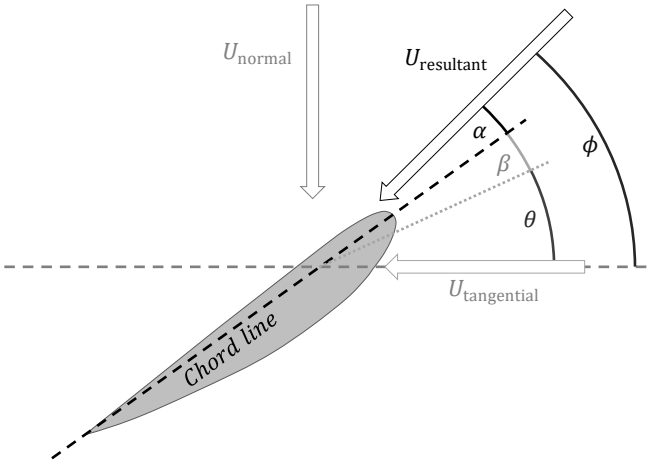

Fig. 2. Diagram illustrating the relationship between the local normal flow speed, U_{normal}, local tangential velocity component, $U_{tangential}$, local resultant flow, $U_{resultant}$, and the local inflow angle, ϕ at a radial cross section of a tidal turbine blade. Also shown is the relationship between local twist angle, θ, blade pitch angle, β, and local angle of attack, α. Blade pitch, β, is the angle between the chord line at the point in time shown and the chord line as installed. Local α decreases as β increases.

This work, however, is focused on developing a passive blade-pitch mechanism which allows the blade to rotate about a bearing at the root, in order to reduce thrust. Such a mechanism should be compatible with blades which exhibit *bend-twist coupling* so that the benefits of both approaches could be combined in future work.

The aim of the passive pitch mechanism portrayed in this study is to allow larger diameter blades to be installed on a tidal turbine, without increasing the forces experienced in high-flow conditions. Power capture is proportional to the square of rotor diameter when all other factors are the same [21], so installing larger blades could increase the annual energy yield of a turbine. To ensure that larger blades enable a greater energy yield, whilst limiting the loads generated by the rotor, the passive pitch mechanism must fulfil the following requirements:

1. In low flow speeds, the blade pitch must be maintained at an optimum angle to maximise coefficient of power.

2. In high flow speeds, the blade pitch angle must increase to ensure that the hydrodynamic loads and power generated by the rotor blades remain within limits.

3. During braking, the blades must pitch in order to reduce the braking torque requirements and to reduce the rotor thrust experienced as the tip speed ratio decreases, which leads to an increase in coefficient of thrust, C_T, as shown in Fig. 3.

D. *Passive blade-pitch mechanism initial design*

The hub size needs to grow in order to accommodate a passive pitch mechanism. For initial design of the passive pitch mechanism portrayed in this study, the decision has been taken to double the hub size compared to that of the fixed pitch turbine. The radius of the blade roots also therefore double as the blade root location is governed by the hub size, as shown in Fig. 4.

II. Mathematical Model

A coupled model has been developed to assist with the development of a passive blade-pitch mechanism.

A hyrodynamic model, the *National Renewable Energy Laboratory*'s (*NREL*) *AeroDyn* tool was used alongside *xfoil* to compute the load distribution generated by a two-bladed tidal turbine rotor. The hydrodynamic model computes a load distribution along the rotor blades for a given operating condition, defined by flow speed, U_∞ and tip speed ratio, λ, and a given pair of blade pitch angles, β_1 and β_2, for the first and second blades respectively.

A mechanical model was developed to predict the pitch response of each blade, based on the characteristics of the passive pitch mechanism and the loads developed by the rotor blades.

The hydrodynamic and mechanical models were then coupled in order to capture the fluid-structure interaction behaviour of the passive pitch mechanism and its impact on the performance of the rotor.

E. *Hydrodynamic model*

AeroDyn, a module of the *NREL*'s *OpenFAST* turbine simulation tool was used to calculate the loads generated by the fluid flow over the rotating tidal turbine rotor blades. *AeroDyn* employs Blade Element Momentum Theory (BEMT) to estimate the effects of flow around the blades by dividing the blade into a series of small radial elements and considering the flow around each element as two-dimensional (2D). *AeroDyn* then then applies correction factors in order to better capture three-dimensional (3D) hydrodynamic effects [22].

The 2D flow data fed into *AeroDyn* consists of lift, drag and moment polars for the hydrofoil at each radial element along the length of the blade. These were generated using *xfoil*, which is based on the linear-vorticity panel method [23].

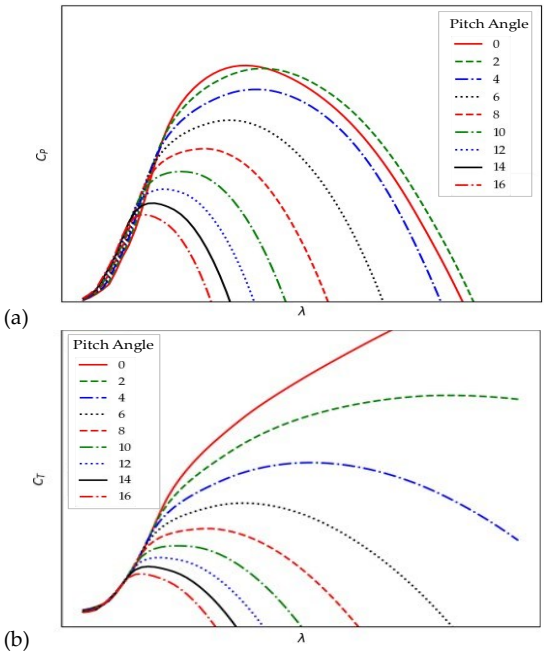

Fig. 3. Typical curves of (a) coefficient of power, C_P, and (b) coefficient of thrust, C_T, against tip speed ratio, λ, for a range of blade pitch angles.

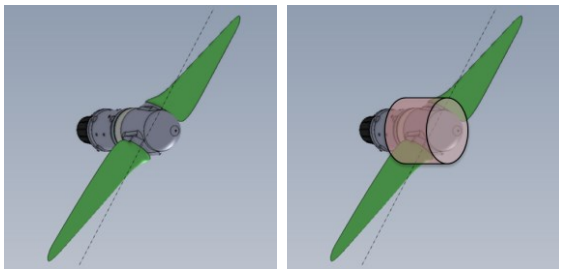

Fig. 4. (a) The original turbine rotor with fixed pitch blades and (b) the rotor with hub enlarged in order to incorporate the passive pitch mechanism.

Drag polars from *xfoil* include the effect of skin friction drag, and are based on the wake momentum thickness far downstream [23].

When using *xfoil* to generate lift, drag and moment polars, an N_{Crit} value of 0.5 was used when simulating turbine performance at a typical tidal site, as empirical date suggests this value is most appropriate [24]. when simulating the loads on the rotor in a tow tank, however, where turbulence levels are very low [25], an N_{Crit} value of 10 was used, which corresponds with clean flow [23]. The results generated by *xfoil* were validated using *OpenFOAM*, a computational fluid dynamics tool, employing a Spalart-Allmaras turbulence model [26].

The correction factors applied by the *AeroDyn* tool include Prandtl's tip-loss and hub-loss models as well as Pitt and Peters model for skewed wake correction in misaligned flow [22].

The hydrodynamic model was validated against experimental data from a 1/6th scale model test at the *Marin* tow tank. The model turbine blades consisted of balanced, symmetric carbon fibre reinforced polymer

(CFRP) laminate which is assumed to be sufficiently rigid to neglect fluid-structure interaction effects.

At each operating condition of interest, the hydrodynamic model was run at pitch increments of 0.25° in order to interpolate the hydrodynamic pitching moment on the first and second blades, M_{H_1} and M_{H_2}, as functions of their respective pitch angle.

F. Mechanical model of passive pitch mechanism

For a given operating condition, defined by flow speed, U_∞, and tip speed ratio, λ, the mechanical model computes the response of the passive pitch mechanism.

The net pitching moment on each blade, which is equal to the blades' polar moment of inertia, J, multiplied by the pitch acceleration of each blade $\ddot{\beta}_1$ and $\ddot{\beta}_2$, is defined by (2) and (3). The net pitching moment on each blade is the sum of the hydrodynamic moment on each blade, M_{H_1} and M_{H_2} respectively, the moment due to damping as a result of the blade rotating in sea water about its pitch axis, M_{D_1} and M_{D_2}, the moment due to friction in the bearings and seals, M_{F_1} and M_{F_2}, and the moment about the pitch axis provided by the passive pitch mechanism, $M_{PP_1}$and M_{PP_2}. These moments are functions of a combination of the pitch rate of each blade, $\dot{\beta}_1$ and $\dot{\beta}_2$ respectively, and the pitch angle of each blade, β_1 and β_2.

$$J\ddot{\beta}_1 = M_{H_1}(\beta_1) + M_{D_1}(\dot{\beta}_1) + M_{F_1}(\dot{\beta}_1, \dot{\beta}_2, \beta_1, \beta_2) + M_{PP_1}(\beta_1, \beta_2) \quad (2)$$

$$J\ddot{\beta}_2 = M_{H_2}(\beta_2) + M_{D_2}(\dot{\beta}_2) + M_{F_2}(\dot{\beta}_1, \dot{\beta}_2, \beta_1, \beta_2) + M_{PP_2}(\beta_1, \beta_2) \quad (3)$$

When the rotor is considered at a steady state, the pitch rate and pitch acceleration of each blade are zero. Equations (2) and (3) then become (4) and (5). The friction term, however, does not disappear, because static friction remains in the bearings and seals.

$$0 = M_{H_1}(\beta_1) + M_{F_1}(\beta_1, \beta_2) + M_{PP_1}(\beta_1, \beta_2) \quad (4)$$

$$0 = M_{H_2}(\beta_2) + M_{F_2}(\beta_1, \beta_2) + M_{PP_2}(\beta_1, \beta_2) \quad (5)$$

A dynamic response, based on (2) and (3), was used to model the loads on the rotor during braking, while a steady-state response, based on (4) and (5), was assumed when analysing the turbine performance at a constant rotor speed in steady flow. This is based on an assumption that the tidal flow speed increases very gradually, while the dynamic impact of shear velocity profile, waves and other turbulence has been neglected.

In the dynamic model, governed by (2) and (3), pitching moment due to friction depends upon the pitch rate of each blade, $\dot{\beta}_1$ and $\dot{\beta}_2$ respectively, as this determines whether the static or dynamic coefficient of friction applies, and in what direction friction applies. The static model, however, neglects the time history of the pitch of each blade and instead applies the static coefficient of friction.

G. Fluid-structure interaction

The hydrodynamic model and mechanical model of the passive pitch mechanism can be coupled such that for a given operating condition, defined by U_∞ and λ, the unique pair of physically feasible blade pitch angles which satisfy both models, β_1 and β_2, can be computed.

The models are coupled such that the outputs from the hydrodynamic model, M_{H_1} and M_{H_2}, form the inputs to the mechanical model, whilst the outputs of the mechanical model, β_1 and β_2, constitute the inputs to the hydrodynamic model, as represented in Fig. 5.

The pair of blade pitch angles which satisfy both the fluid and structural elements of the model were found by solving (2) and (3) simultaneously. For dynamic simulations, the coupled model must be solved at each time-step.

III. Modelling Results

H. Validation of hydrodynamic model

The turbine operates at the tip speed ratio which corresponds with maximum power extraction, λ^*, until the generator torque or power limits are reached. The turbine subsequently operates at higher tip speed ratios.

Fig. 6 (a) and (b) show generally good agreement for coefficients of power and torque between the hydrodynamic model and results data from a scale model test conducted in a tow tank. The hydrodynamic model does, however, predict greater coefficients of power and thrust for tip speed ratios below λ^*.

The disparity between the model and the experimental data partly stems from the fact that BEMT and *xfoil* cannot capture the effect of flow separation at high angles of attack which occur at low tip speed ratios [27].

Disparity between the model and experimental data could also be due to the application of zig-zag tape on the test model blades. Zig-zag tape was applied to promote transition to turbulent flow, in order to simulate the effects of higher Reynolds number flow compared to the true Reynolds number at 1/6th scale. Zig-zag tape may, however, have altered the lift and drag generated by the blades in a manner that has not been captured by the hydrodynamic model.

Geometric errors in the blades of the scale model manufactured may also have resulted in disparity between the model and experimental results.

Blockage and edge effects should not have contributed significantly to disparity between experimental and modelling results as the blockage ratio for the scale model in the tow tank was just 6%, while the hub was one full rotor diameter below the surface and over six full rotor diameters above the tank floor.

Turbulence is also unlikely to have resulted in disparity between the model and experimental data as very low turbulence levels can be achieved in the tow tank if sufficient settling time is allowed between runs [28], which is reflected in the choice of N_{Crit} value.

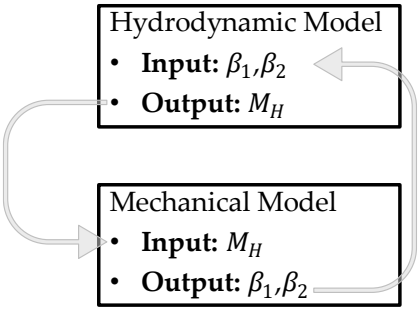

Fig. 5. Flow diagram representing the coupling of the hydrodynamic and mechanical models in order to capture fluid-structure interaction.

Fig. 6 (c) shows that the thrust values from the hydrodynamic model and the experimental data for tip speed ratios are within 3% for tip speed ratios greater than that which corresponds to maximum power extraction, λ^*. This is important as the response of the passive pitch mechanism is influenced by the hydrodynamic loads generated by the rotor blades.

I. Effect of passive pitch mechanism on rotor thrust

As stated in Section C, the aim of the passive pitch mechanism developed in this study is to reduce the thrust force on the rotor in high-flow conditions, including when braking. This will then allow a larger diameter rotor to be installed without increasing the maximum thrust experienced during operation when compared to the rotor with fixed pitch blades.

For a rotor with fixed pitch blades, the maximum thrust force, T^*, is experienced when operating at cut-out flow speed, U^*. This is equal to the thrust force experienced at the beginning of the braking process.

When the blades are fitted to a passive pitch mechanism, however, the maximum thrust force is experienced during braking because as the pitch angle increases, the peak of the coefficient of thrust curve shifts towards lower tip speed ratio values, as shown in Fig. 3 (b). The coefficient of thrust therefore increases as the rotor speed decreases, as happens during braking, when the blades are in a pitched position.

Fig. 7 shows the thrust force generated by both fixed pitch and passive pitch rotors during braking, as computed by the model developed as part of this study. It can be seen that the passive pitch mechanism reduces the maximum rotor thrust by over 50%.

There is scope to scale up the rotor blades of the turbine incorporating passive pitch control until the maximum thrust force experienced during braking is equal to the maximum thrust force exerted on the rotor with fixed pitch blades.

Fig. 8 shows that when the passive pitch mechanism is incorporated, assuming that the turbine rotor and passive pitch mechanism can be scaled geometrically, the rotor diameter could be scaled up by a factor of up to 1.42 without increasing the maximum thrust load experienced.

Three turbines will be referred to throughout the remainder of this work:

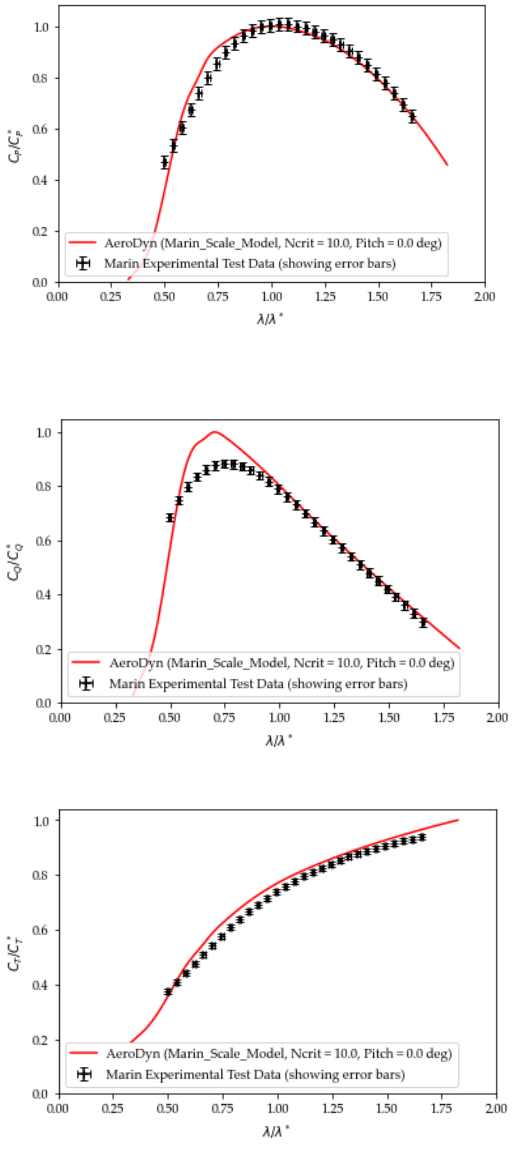

Fig. 6. Comparison of (a) Coefficient of Power, C_P, (b) Coefficient of Torque, C_Q, and (c) Coefficient of Thrust, C_T, data from experimental tests for a rotor with rigid blades and the AeroDyn hydrodynamic model, uncoupled form the mechanical model. Performance coefficients are normalised relative to the maximum value computed by the model for the range shown in each figure. Tip speed ratio, λ, is normalised relative to the tip speed ration which corresponds with maximum C_P, λ^*. The coefficients of power, torque and thrust, are normalised relative to the maximum coefficients of power, torque and thrust predicted by the hydrodynamic model within this range of tip speed ratios, C_P*, C_Q* and C_T* respectively.

Turbine A: Fixed blade-pitch, original-scale hub and rotor diameter

Turbine B: Passive blade-pitch, hub geometry doubled, original-scale rotor diameter

Turbine C: Passive blade-pitch, hub geometry increased by factor of 2.8, rotor diameter scaled by factor of 1.4

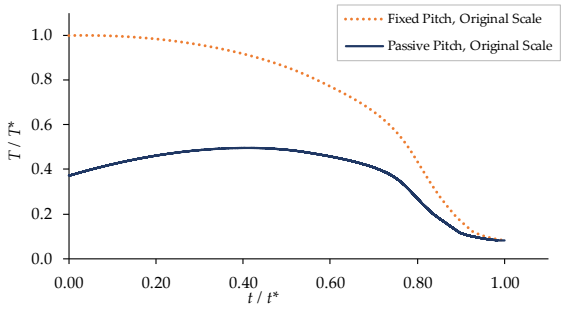

Fig. 7. Modelled thrust force during braking for a fixed pitch tidal turbine compared to a turbine with the same rotor diameter incorporating a passive pitch mechanism. Rotor thrust, T, is normalised relative to the maximum thrust that the rotor with fixed pitch blades would experience, T^*. Time, t, is normalised relative to the total time taken to fully brake the rotor, t^*.

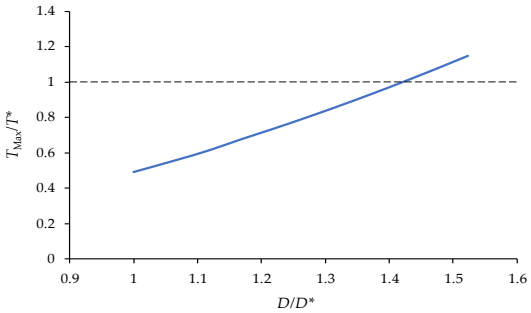

Fig. 8. The relationship between maximum thrust predicted by the model and rotor diameter, assuming that the blade geometries are all geometrically similar, that the passive pitch mechanism scales with rotor diameter, and that all limits, including power limit, torque limit and cut-out flow speed, remain the same. Maximum rotor thrust, T_{Max}, is normalised relative to the maximum thrust that the rotor with fixed pitch blades would experience, T^*. Rotor diameter, D, is normalised relative to the diameter of the original-scale rotor with fixed pitch blades, D^*.

It is very important to note the caveat that the modelled performance of Turbine C in this work represents a target for a turbine with a passive blade-pitch mechanism, based on an initial design. It does not represent the predicted performance of a production turbine based on detailed design.

J. *Effect of passive pitch mechanism and scaled-up rotor on power capture*

Fig. 9 (a) shows that the average power generated by Turbine C is higher than that of Turbine A for flow speeds up to 0.70 of cut-out flow. All power curves flatten off at the generator power limit.

Fig. 9 (b) shows that the thrust exerted Turbine C is higher than that exerted on Turbine A for low flow speeds, but lower than that exerted on the Turbine A in high-flow conditions. This is because the passive pitch mechanism leads to a predicted decreased in thrust in flows above 0.70 of cut-out speed. This unexpected result appears to be due to the model predicting that as the pitch angle increases, the angle of attack at each hydrofoil along the length of the blades decreases, as illustrated in Fig. 1, which, according to *xfoil*, results in an increased coefficient of moment, C_{M}.

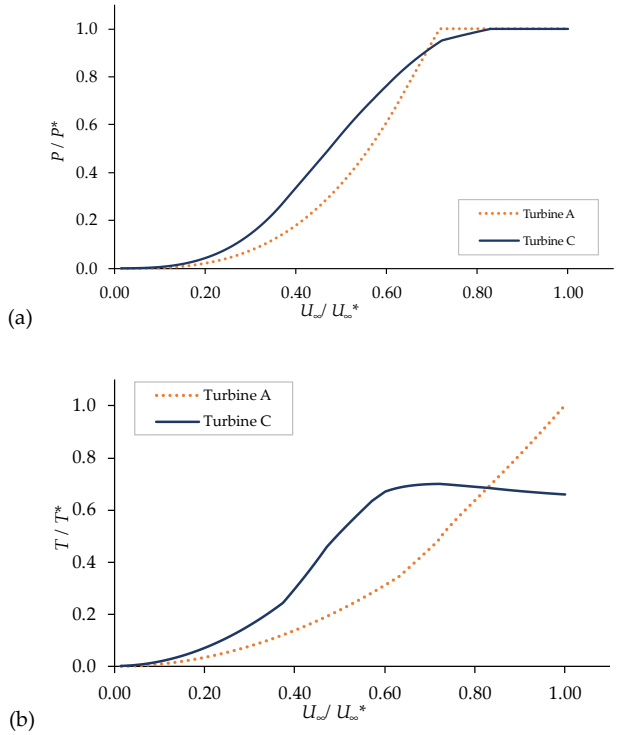

Fig. 9. (a) Average rotor power and (b) rotor thrust against flow speed for Turbine A compared to Turbine B. Rotor power, P, is normalised relative to the generator power limit, P^*. Rotor thrust, T, is normalised relative to the maximum thrust that the rotor with fixed pitch blades would experience, T^*. Flow speed, U_∞, is normalised relative to U_∞^*, the cut-out flow speed for the turbine studied here. Note that the average power is calculated as the mean of the power output in gradually increasing and decreasing flow speeds.

K. *Effect of friction on the passive pitch mechanism*

Fig. 10 shows the effect that friction within the passive pitch mechanism has on the power generated by Turbine C. A hysteresis effect can be seen; for any given flow speed, the turbine generates more power when the flow speed, and therefore the loads on the rotor blades, are gradually increasing compared to when they are decreasing. This result is due to the fact that when the flow speed and loads on the rotor blades are increasing, friction acts to prevent the blade pitch angle from increasing. This means that the blades experience a higher angle of attack, and so generate greater lift and drag forces, resulting in more torque and therefore more power. When the flow speed is decreasing, the opposite is true, so the rotor experiences lower loads and captures less power.

It has been assumed throughout this study that a relatively low coefficient of friction can be achieved for components within the passive pitch mechanism. Though it must be stressed that the performance of Turbine C therefore represents a target rather than a prediction for a production turbine with a passive pitch mechanism.

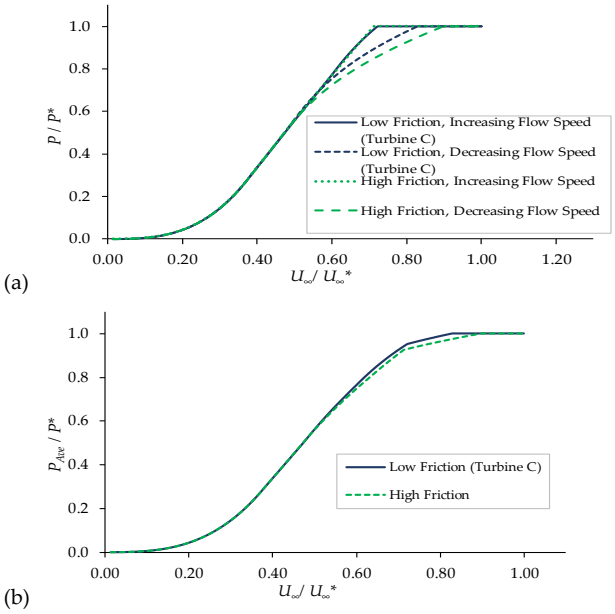

Fig. 10. (a) Plot of instantaneous power against flow speed comparing the performance of Turbine C compared to an identical turbine with greater friction within the passive pitch mechanism, when flow speed is increasing and decreasing at a sufficiently slow rate that the system can be considered at a steady state. (b) Plot of average power against flow speed comparing the performance of Turbine C compared to an identical turbine with greater friction within the passive pitch mechanism. Note that the average power is calculated as the mean of the power output in gradually increasing and decreasing flow speeds. Instantaneous rotor power, P, and average rotor power, P_{Ave}, are normalised relative to the generator power limit, P^*. Flow speed, U_∞, is normalised relative to U_∞^*, the cut-out flow speed for the turbine studied here.

L. *Effect of passive pitch mechanism effectiveness on turbine performance*

An ideal passive pitch mechanism would match the pitch response of an active pitch system in order to achieve the objectives laid out in Section C. The blades would remain at their optimal pitch angle until the generated power limit is reached, resulting in a maximum coefficient of power in low-flow conditions. The blades would then *pitch-to-feather* at a relatively high rate as the flow speed increases further, resulting in reduced loads in high-flow conditions.

Fig. 11 shows that a highly effective passive pitch mechanism, which corresponds to Turbine C modelled throughout this study, would come close to matching the performance that can be achieved with active pitch control. The power generated by Turbine C only deviates from the power output that could be achieved by a turbine with active pitch control between 0.55 and 0.85 of the cut-out flow speed.

Fig. 11 shows that less effective passive pitch mechanisms would cause the blades to begin pitching at lower flow speeds, such that the power curves deviate from that of the turbine with active pitch control. Again, it must be stressed that the modelled performance of Turbine C represents a target rather than a prediction.

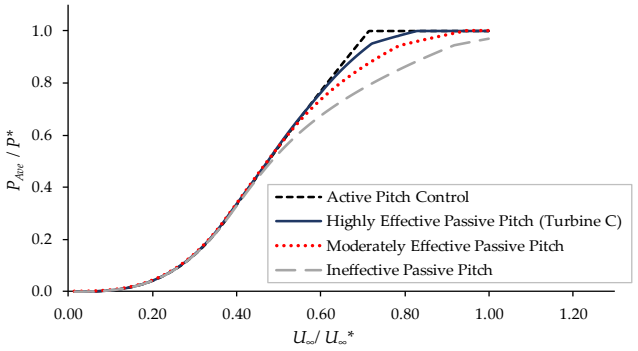

Fig. 11. Plot of average power against flow speed comparing the performance of a scaled-up turbine with active pitch control, and passive pitch control with highly effective, moderately effective and ineffective mechanisms. Note that the average power is calculated as the mean of the power output in gradually increasing and decreasing flow speeds.

M. *Blade pitch response predicted by modelling*

Fig. 12 shows that the passive pitch mechanism holds both blades at 0° pitch, which corresponds with maximum coefficient of power, until 0.47 of cut-out flow speed, regardless of whether the flow speed is increasing or decreasing.

Fig. 12 then shows that the blades pitch less for any given flow speed when the flow speed is gradually increasing compared to when it is decreasing. This occurs because friction acts to reduce the pitch angle of each blade in accelerating flow, whereas when the flow speed decreases, friction inhibits the extent to which the blades return to their original angle from their pitched position.

It can also be observed in Fig. 12 that the pitch angle of the two blades differ from one another. This is also due to friction within the bearings and seals of the passive pitch mechanism which is captured by the mechanical model.

Fig. 13 shows how the pitch angle of each blade changes during braking, according to a dynamic model governed by (2) and (3). The model suggests that friction within the mechanism prevents the blades from pitching further during braking, and further reducing the thrust load on the rotor.

N. *Energy yield gains from incorporating passive pitch*

Fig. 14 (a) shows a typical tidal flow distribution based on data from [29], as well as the power curves for both Turbine A and Turbine C. Turbine C captures more power for all flow speeds up to 0.75 of the cut-out flow speed.

The annual energy yield has been computed by calculating the energy generated in each flow speed bin. Each bin is defined by an upper and lower limit of flow speed, 0.1 m/s apart. Fig. 14 (b) shows that the energy captured by Turbine C is greater for all bins below 0.75 of the cut-out speed. Turbine A, with fixed pitch blades, captures more power between 0.75 and 0.90 of cut-out flow speed, but these conditions are experienced less than 5% of the time so this contributes very little energy yield.

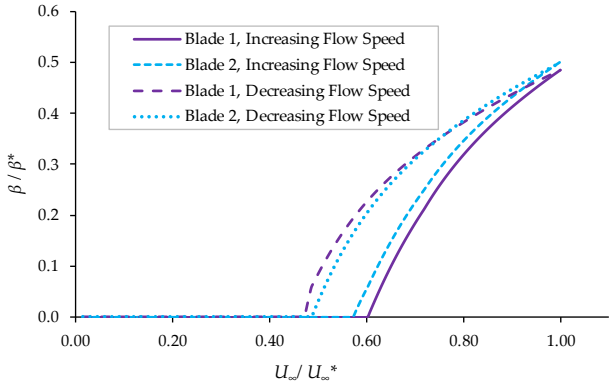

Fig. 12. Blade pitch angle against flow speed for Turbine C. Blade pitch, β, is normalised relative to the maximum blade pitch allowed by the passive pitch mechanism, β^*. Flow speed, U_∞, is normalised relative to $U_\infty{}^*$, the cut-out flow speed for the turbine studied here.

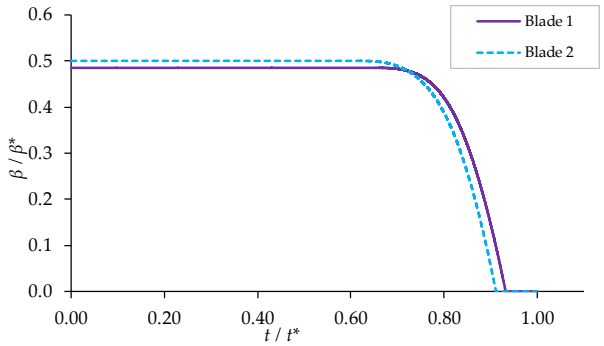

Fig. 13. The passive pitch response of each blade during braking at cut-out flow speed. Blade pitch, β, is normalised relative to the maximum blade pitch allowed by the passive pitch mechanism, β^*. Time, t, is normalised relative to the total time taken to fully brake the rotor, t^*.

Fig. 14 (c) then shows the increased cumulative energy generated by Turbine C compared to Turbine A. The increase in annual energy yield based on the given flow speed distribution is shown to be 32.7%.

IV. Conclusion

A passive blade-pitch mechanism has the potential to reduce the LCOE for tidal energy, by increasing energy yield compared to smaller turbines with fixed pitch blades, whilst avoiding the capital and maintenance costs associated with active pitch mechanisms.

An ideal passive pitch mechanism would provide a high resistance to blade-pitch in low-flow conditions, followed by a relatively low resistance to blade-pitch above the flow speed at which the generator power limit is reached.

An ideal passive pitch mechanism would also be carefully designed in order to minimise friction such that the blades respond rapidly to changes in load, and such that the blades increasingly *pitch-to-feather* as thrust increases, even if the rotor speed decreases.

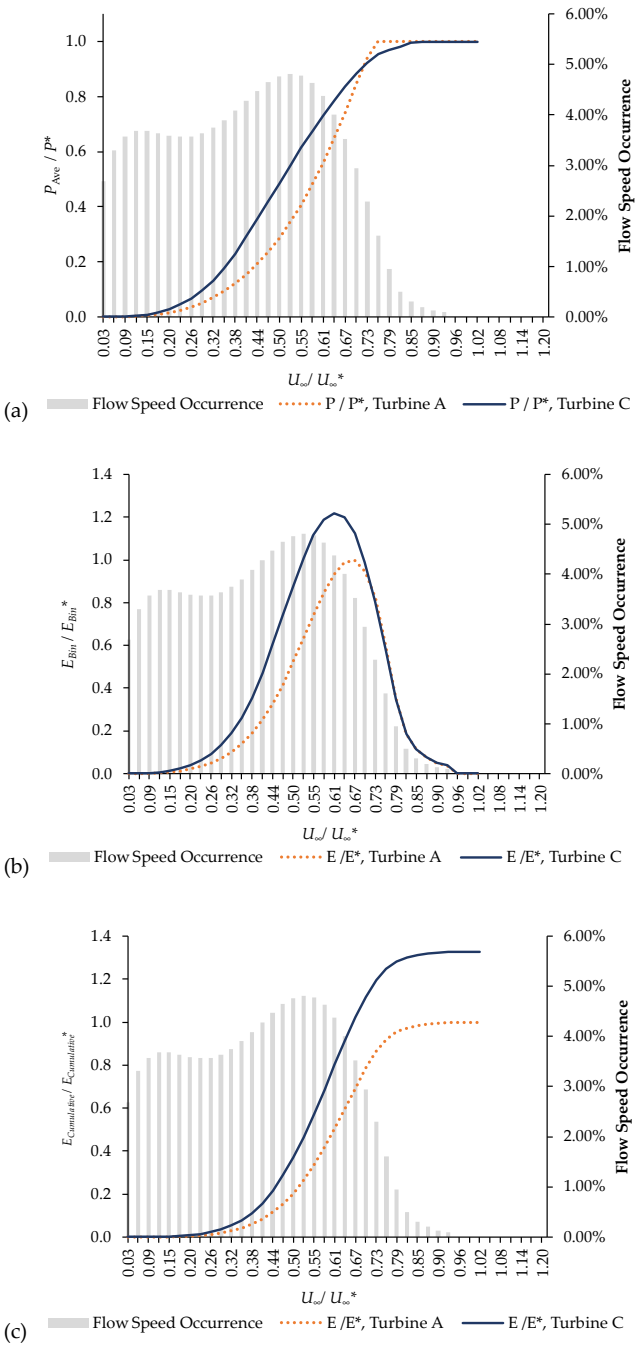

Fig. 14. Comparison of (a) average power, P_{Ave}, (b) energy generation per flow speed bin, E_{Bin}, and (c) cumulative energy generation, $E_{\text{Cumulative}}$, against flow speed for Turbine A compared to Turbine C. Average power, P_{Ave}, is normalised relative to the generator power limit, P^*. Energy generation per flow speed bin, E_{Bin}, is normalised relative to the energy generation in the most productive bin for the turbine with fixed pitch blades, $E_{Bin}{}^*$. Cumulative energy generation, $E_{\text{Cumulative}}$, is normalised relative to the cumulative annual energy yield for the turbine with fixed pitch blades, $E_{Cumulative}{}^*$. All three plots are overlayed against a typical flow speed distribution [29] which has been used to estimate energy generation.

Minimising friction would allow both blade-pitch angles to increase during braking, as opposed to staying relatively constant as shown in Fig. 11, in order to reduce thrust during braking compared to the thrust acting on the rotor with passive blade-pitch shown in Fig. 7.

Reducing friction would also shrink the hysteresis effect between power curves for increasing and decreasing flow speeds, as seen in Fig. 12 (a). This would increase the average power generated at each flow speed, ash shown in Fig. 12 (b).

Friction is also responsible for the blade pitch imbalance, the difference in pitch angles between the two blades as seen in Figs. 9 and 10. Reducing friction could also help to avoid potential problems associated with this imbalance.

V. Further Work

Detailed design work needs to be undertaken in order to realise the potential benefits described in this study of implementing a passive pitch mechanism.

Further analysis is also needed to check whether the blade pitch imbalance is problematic. A dynamic analysis of the response of the passive pitch mechanism to flow speed variations due to shear profile, waves or flow misalignment is required.

Physical testing will also be required in order to validate the modelling work on the passive pitch mechanism.

References

[1] S. Walker and P. R. Thies, "A review of component and system reliability in tidal turbine deployments," *Renew. Sustain. Energy Rev.*, vol. 151, p. 111495, Nov. 2021, doi: 10.1016/J.RSER.2021.111495.

[2] J. Thake, "DEVELOPMENT, INSTALLATION AND TESTING OF A LARGE SCALE TIDAL CURRENT TURBINE," Reading, UK, Oct. 2005.

[3] B. Hu and C. F. W. Stock-Williams, "Operations & Maintenance Simulation for Tidal Energy Converters," Petten, The Nethelands, 2018.

[4] C. M. Johnstone, D. Pratt, J. A. Clarke, and A. D. Grant, "A techno-economic analysis of tidal energy technology," *Renew. Energy*, vol. 49, pp. 101–106, Jan. 2013, doi: 10.1016/J.RENENE.2012.01.054.

[5] M. Lewis, S. P. Neill, P. Robins, M. R. Hashemi, and S. Ward, "Characteristics of the velocity profile at tidal-stream energy sites," *Renew. Energy*, vol. 114, pp. 258–272, Dec. 2017, doi: 10.1016/J.RENENE.2017.03.096.

[6] E. A. Bossanyi, "Wind Turbine Control for Load Reduction," *Wind Energy*, vol. 6, no. 3, pp. 229–244, Jul. 2003, doi: 10.1002/WE.95.

[7] Z. Zhou *et al.*, "Control Strategies for Tidal Stream Turbine Systems-A Comparative Study of ADRC, PI, and High-Order Sliding Mode Controls. Control Strategies for Tidal Stream Turbine Systems-A Comparative Study of ADRC, PI, and High-Order Sliding Mode Controls Control Strategies for Tidal Stream Turbine Systems-A Comparative Study of ADRC, PI, and High-Order Sliding Mode Controls," in *45th Annual Conference of the IEEE Industrial Electronics Society*, Oct. 2019, pp. 6981–6986, doi: 10.1109/IECON.2019.8927629ï.

[8] M. Arnold, F. Biskup, and P. W. Cheng, "Load reduction potential of variable speed control approaches for fixed pitch tidal current turbines," *Int. J. Mar. Energy*, vol. 15, pp. 175–190, Sep. 2016, doi: 10.1016/J.IJOME.2016.04.012.

[9] S. Baleriola, A. Leroy, S. Loyer, P. Devinant, and S. Aubrun, "Experimental lift control using fluidic jets on a model wind turbine," *J. Phys. Conf. Ser.*, vol. 1037, no. 2, Jun. 2018, doi: 10.1088/1742-6596/1037/2/022014.

[10] B. Whitby and C. E. Ugalde-Loo, "Performance of Pitch and Stall Regulated Tidal Stream Turbines," *IEEE Trans. Sustain. ENERGY*, vol. 5, no. 1, 2014, doi: 10.1109/TSTE.2013.2272653.

[11] X. Yin and X. Zhao, "Composite Hierarchical Pitch Angle Control for a Tidal Turbine Based on the Uncertainty and Disturbance Estimator," *IEEE Trans. Ind. Electron.*, vol. 67, no. 1, 2020, doi: 10.1109/TIE.2019.2896261.

[12] I. Benson, C. Frost, I. Benson, P. Jeffcoate, B. Elsäßer, and T. Whittaker, "The Effect of Control Strategy on Tidal Stream Turbine Performance in Laboratory and Field Experiments," *Energies*, vol. 11, no. 6, 2018, doi: 10.3390/en11061533.

[13] A. Garanovic, "SIMEC Atlantis makes progress on novel variable pitch system for 2MW tidal turbines," *Offshore Energy*, Dec. 08, 2021. https://www.offshore-energy.biz/simec-atlantis-makes-progress-on-novel-variable-pitch-system-for-2mw-tidal-turbines/ (accessed May 17, 2023).

[14] T. K. Barlas and G. A. M. van Kuik, "Review of state of the art in smart rotor control research for wind turbines," *Prog. Aerosp. Sci.*, vol. 46, no. 1, pp. 1–27, Jan. 2010, doi: 10.1016/J.PAEROSCI.2009.08.002.

[15] EPRI, "Estimation of Turbine Reliability Figures within the DOWEC Project," Washington, D.C., USA, 2016. [Online]. Available: https://www.ecn.nl/fileadmin/ecn/units/wind/docs/dowec/10048_004.pdf.

[16] Y. Lin, L. Tu, H. Liu, and W. Li, "Fault analysis of wind turbines in China," *Renew. Sustain. Energy Rev.*, vol. 55, pp. 482–490, Mar. 2016, doi: 10.1016/J.RSER.2015.10.149.

[17] System Performance Availability and Reliability Trend Analysis (SPARTA), "Portfolio Review 2016," Northumberland, UK, 2016.

[18] R. F. Nicholls-Lee, S. R. Turnock, and S. W. Boyd, "Application of bend-twist coupled blades for horizontal axis tidal turbines," *Renew. Energy*, vol. 50, pp. 541–550, Feb. 2013, doi: 10.1016/J.RENENE.2012.06.043.

[19] K. E. Porter *et al.*, "Flume testing of passively adaptive composite tidal turbine blades under combined wave and current loading," *J. Fluids Struct.*, vol. 93, Feb. 2020, doi: 10.1016/J.JFLUIDSTRUCTS.2019.102825.

[20] P. Jeffcoate, R. Starzmann, B. Elsaesser, S. Scholl, and S. Bischoff, "Field measurements of a full scale tidal turbine," *Int. J. Mar. Energy*, vol. 12, pp. 3–20, Dec. 2015, doi: 10.1016/J.IJOME.2015.04.002.

[21] D. Coles *et al.*, "A review of the UK and British Channel Islands practical tidal stream energy resource," *Proc. R. Soc. A*, vol. 477, Oct. 2021, doi: 10.1098/rspa.2021.0469.

[22] J. M. Jonkman, G. J. Hayman, B. J. Jonkman, R. R. Damiani, and R. E. Murray, "AeroDyn v15 User's Guide and Theory Manual," Goloden, USA, 2017.

[23] M. Drela and H. Youngren, "XFOIL 6.9 User Primer," *MIT*, Nov. 30, 2001. https://web.mit.edu/drela/Public/web/xfoil/xfoil_doc.txt (accessed May 26, 2023).

[24] S. A. El-Shahat, G. Li, F. Lai, and L. Fu, "Investigation of parameters affecting horizontal axis tidal current turbines modeling by blade element momentum theory," *Ocean Eng.*, vol. 202, p. 107176, Apr. 2020, doi: 10.1016/J.OCEANENG.2020.107176.

[25] L. Luznik, M. van Benthem, K. Flack, and E. Lust, "Tow tank measurements of turbulent flow in the near wake of a horizontal axis marine current turbine under steady and unsteady inflow conditions," 2013. [Online]. Available: https://ui.adsabs.harvard.edu/abs/2013APS..DFDA13002L/abstract.

[26] M. N. Doan, I. H. Alayeto, K. Kumazawa, and S. Obi, "Computational fluid dynamic analysis of a marine hydrokinetic crossflow turbine in low Reynolds number flow," in *ASME-JSME-KSME Joint Fluids Engineering Conference 2019*, Jul. 2019, vol. 2, doi: 10.1115/AJKFLUIDS2019-4698.

[27] U. Boatto, P. A. Bonnet, F. Avallone, and D. Ragni, "Momentum Theory-based engineering models for wind turbine rotors under uniform steady inflow," *Renew. Energy*, vol. 214, pp. 307–317, 2023, [Online]. Available: https://www.sciencedirect.com/science/article/abs/pii/S0960148123005001.

[28] M. Jentzsch, H. J. Schmidt, R. Woszidlo, C. N. Nayeri, and C. O. Paschereit, "Challenges and procedures for experiments with steady and unsteady model velocities in a water towing tank," *Exp. Fluids*, vol. 62, no. 4, pp. 1–20, Apr. 2021, doi: 10.1007/S00348-021-03151-5/FIGURES/15.

[29] M. Liu, W. Li, R. Billinton, C. Wang, and J. Yu, "Modeling tidal current speed using a Wakeby distribution," *Electr. Power Syst. Res.*, vol. 127, pp. 240–248, Oct. 2015, doi: 10.1016/J.EPSR.2015.06.014.